IEEE Control Systems Letters paper presented at
2024 IEEE 63rd Conference on Decision and Control (CDC)
December 16-19, 2024. MiCo, Milan, Italy

Sampled-data Circular Path Following Control of Four Wheeled Mobile Robots with Steering Angle Saturation

Hitoshi Katayama[1], Kohei Hayashi[2] and Yuya Imamura[3]

***Abstract*— Sampled-data circular path following control of four wheeled mobile robots with steering angle saturation is considered. The line-of-sight guidance algorithm is used to drive a tracking error dynamics and sampled-data path following control is formulated as sampled-data stabilization of a tracking error dynamics. Both single-rate and multi-rate sampled-data steering angle controllers are designed on the basis of the Euler model of a tracking error dynamics. The closed-loop tracking error dynamics given by designed controllers is represented by a cascade system with the disturbance input induced by steering angle saturation. Then we show that designed controllers achieve sampled-data circular path following control in the semiglobally practically input-to-state stable sense. Simulation and experimental results are also given to show the effectiveness of designed controllers.**

I. INTRODUCTION

Design of control systems of wheeled robots has been actively discussed from a wide range of applications such as automatic driving, formation driving, and cooperative operations ([1], [2]). In particular, trajectory tracking and path following control of wheeled robots is very important. Several design methods of path following controllers based on energy shaping through immersion and invariance [3], sliding mode path following [4], transverse feedback linearization (TFL) [5] among others have been proposed for mechanical systems including wheeled robots. A guidance algorithm called the line-of-sight (LOS) method has been developed for trajectory tracking control of vessels [6]. It has been applied for straight-line and circular path following control and formation control of surface vessels ([7], [8]). It has been also used for path following control problems of wheeled robots [9]. Digital computers with A/D and D/A converters are usually used to control continuous-time plants in modern control systems and such control systems are called sampled-data systems ([10], [11]). Sampled-data motion planning under multi-rate discrete-time control has been introduced [12] and then single-rate and multi-rate path following discrete-time controllers based on TFL has been considered for sampled-data car-like mobile robots [13]. The LOS guidance algorithm has been also used to design straight-line tracking controllers for sampled-data underactuated surface vessels [14].

[1]Hitoshi Katayama is with Department of Mechanical System Engineering, The University of Shiga Prefecture, 522 8533 Hikone-City, Japan katayama.h@mech.usp.ac.jp

[2]Kohei Hayashi is with Department of Mechanical System Engineering, The University of Shiga Prefecture, 522 8533 Hikone-City, Japan tz22khayashi@ec.usp.ac.jp

[3]Yuya Imamura is with Department of Mechanical System Engineering, The University of Shiga Prefecture, 522 8533 Hikone-City, Japan oe22yimamura@ec.usp.ac.jp

In this paper we consider sampled-data circular path following control of a four wheeled mobile robot with steering angle saturation, since a combination of circular paths and straight-lines is sometimes used to approximate a general path and it is also used for way-point guidance [15]. We apply the LOS guidance algorithm to design discrete-time controllers that achieve circular path following. First, we introduce a control model of a four wheeled mobile robot and a desired circular path. Then we define a cross-track error and a tracking error of the attitude of the robot by using the LOS guidance algorithm. Here we assume that the control input is realized through a zero-order hold. In this case, sampled-data circular path following control is formulated as sampled-data stabilization of a tracking error dynamics. Then we use the Euler model of a tracking error dynamics to design both single-rate and multi-rate sampled-data steering angle controllers. Due to steering angle saturation, a closed-loop tracking error dynamics given by a designed controller is represented by a cascade system with the disturbance input induced by steering angle saturation. Then we show that a sampled-data closed-loop tracking error dynamics is semiglobally practically input-to-state stable (SP-ISS). We also compare the proposed control approach to those presented in [9] and [13]. Finally, simulation and experimental results are given to show both the effectiveness of designed controllers and the dependence of a length of sampling periods to control performance.

Notation: Let $\mathbf{N}_0 = \{0, 1, 2, ..\}$ and $\mathbf{R}_{\geq 0}$ a set of nonnegative real numbers. For $x = [\, x_1 \quad ... \quad x_n \,]^T \in \mathbf{R}^n$ let $|x| = \sum_{i=1}^n |x_i|$. Let $\mathcal{K}$ be a class of functions $\alpha : \mathbf{R}_{\geq 0} \to \mathbf{R}_{\geq 0}$ that are zero at zero and strictly increasing, and $\mathcal{K}_\infty$ a class of functions $\alpha \in \mathcal{K}$ satisfying $\lim_{r\to\infty} \alpha(r) = \infty$. Let $\mathcal{KL}$ be a class of functions β: $\mathbf{R}_{\geq 0} \times \mathbf{R}_{\geq 0} \to \mathbf{R}_{\geq 0}$ that satisfy $\beta(s, t) \in \mathcal{K}$ for fixed $t \geq 0$ and $\lim_{t\to\infty} \beta(s, t) = 0$ for each fixed $s \geq 0$ [16]. For simplicity of notation, we write $x(t)$ and $x[k]$ to show continuous-time and discrete-time signals, respectively and $f(\eta_1(\cdot), \eta_2(\cdot)) = f(\eta_1, \eta_2)(\cdot)$.

II. PRELIMINARY RESULTS

Consider

$$\dot{\xi} = f(\xi, u, v) \tag{1}$$

where $\xi \in \mathbf{R}^n$ is the state, $u \in \mathbf{R}^m$ is the control input realized through a zero-order hold, i.e., $u(t) = u(kT) =: u[k]$ for any $t \in [kT, (k + 1)T)$, $v \in \mathbf{R}^{n_v}$ is the external disturbance, and $T > 0$ is an input sampling period. Here we assume that f is locally Lipschitz and satisfy $f(0, 0, 0) = 0$. Let $v(t) = v(kT) =: v[k]$ for any $t \in [kT, (k + 1)T)$.

Then for each initial state $\xi(0)$ and constant inputs, we assume the existence of a unique solution $\xi(t)$ of the system (1) defined on some finite interval $[0, t_1)$. The difference equations corresponding to the exact (discretized) model and the Euler (approximate) model of the system (1) are given, respectively by

$$\xi[k+1] = F_T^e(\xi, u, v)[k], \quad (2)$$
$$\xi[k+1] = F_T^E(\xi, u, v)[k] \quad (3)$$

where $F_T^e(\xi, u, v)[k] = \xi[k] + \int_{kT}^{(k+1)T} f(\xi(t), u[k], v[k])dt$ and $F_T^E(\xi, u, v) = \xi + Tf(\xi, u, v)$. Here note that $\xi[k] = \xi(kT)$ for the exact model (2) and $T > 0$ is a design parameter that can be assigned arbitrarily. A state feedback controller $u[k] = u_T(\xi[k])$ that is parameterized by $T > 0$, is designed on the basis of the Euler model (3). In this case, the closed-loop systems (2) and (3) with $u[k] = u_T(\xi[k])$ are given by

$$\xi[k+1] = F_T^i(\xi, u_T(\xi), v)[k] \quad (4)$$

for $i = e$ and $i = E$, respectively. Let $\|v\|_\infty = \sup_{s\in\mathbf{N}_0} |v[s]|$. If $\|v\|_\infty < \infty$, then we write $v \in l_\infty$.

Definition 2.1: [17] 1) The system (4) is SP-ISS if there exist $\beta \in \mathcal{KL}$ and $\gamma \in \mathcal{K}$ such that for any positive real numbers (D_ξ, D_v, d) there exists $T^* > 0$ such that the solutions of the system (4) satisfy $|\xi[k]| \le \beta(|\xi[0]|, kT) + \gamma(\|v\|_\infty) + d$ for any $k \in \mathbf{N}_0$, $T \in (0, T^*)$, $\xi[0] \in \mathbf{R}^n$ with $|\xi[0]| \le D_\xi$, and $v \in l_\infty$ with $|v| \le D_v$.

2) The system (4) with $v[\cdot] = 0$ is semiglobally practically asymptotically stable (SPAS) if there exists $\beta \in \mathcal{KL}$ such that for any positive real numbers (D_ξ, d), there exists $T^* > 0$ such that the solutions of the system (4) with $v[\cdot] = 0$ satisfy $|\xi[k]| \le \beta(|\xi[0]|, kT) + d$ for any $k \in \mathbf{N}_0$, $T \in (0, T^*)$, and $\xi[0] \in \mathbf{R}^n$ with $|\xi[0]| \le D_\xi$.

Definition 2.2: [17] Let $\hat{T} > 0$ be given and $V_T : \mathbf{R}^n \to \mathbf{R}_{\ge 0}$ defined for each $T \in (0, \hat{T})$. The system (4) is called Lyapunov-SP-ISS, if there exist $\alpha_i \in \mathcal{K}_\infty$, $i = 1, 2, 3$ and $\gamma \in \mathcal{K}$ such that for any positive real numbers (D_1, D_2, d), there exist T^* and $L > 0$ such that $\alpha_1(|\xi|) \le V_T(\xi) \le \alpha_2(|\xi|)$, $V_T(F_T^i(\xi, u_T(\xi), v)) - V_T(\xi) \le T[-\alpha_3(|\xi|) + \gamma(||v||_\infty) + d]$, and $|V_T(\xi_1) - V_T(\xi_2)| \le L|\xi_1 - \xi_2|$ for any $T \in (0, T^*)$, ξ, ξ_1, $\xi_2 \in \mathbf{R}^n$ with $\max\{|\xi|, |\xi_1|, |\xi_2|\} \le D_1$, and $v \in l_\infty$ with $|v| \le D_2$.

Definition 2.3: [17] $u_T(\xi)$ is locally uniformly bounded if for any $D_\xi > 0$, there exist $T^* > 0$ and $D_u > 0$ such that $|u_T(\xi)| \le D_u$ for any $T \in (0, T^*)$ and $\xi \in \mathbf{R}^n$ with $|\xi| \le D_\xi$.

We need the following assumption [18].

A1: There exist γ_1, $\gamma_2 \in \mathcal{K}_\infty$ and k, $R > 0$ such that $|f(\xi, u, v)| \le k|\xi| + \gamma_1(|u|) + \gamma_2(|v|)$ for any $\xi \in \mathbf{R}^n$, $u \in \mathbf{R}^m$, $v \in \mathbf{R}^{n_v}$ satisfying $\max\{|\xi|, |u|, |v|\} \le R$.

Theorem 2.1: ([17], [18]) Assume that the Euler model (4) is Lyapunov-SP-ISS and $u_T(\xi)$ is locally uniformly bounded. Then the exact model (4) is SP-ISS. Moreover, if **A1** is satisfied, then the closed-loop sampled-data system (1) with $u[k] = u_T(\xi(kT))$ for any $t \in [kT, (k+1)T)$ and $k \in \mathbf{N}_0$ is SP-ISS, i.e., there exist $\beta \in \mathcal{KL}$ and $\gamma \in \mathcal{K}$ such that for any positive real numbers (D_x, D_v, d) there exists $T^* > 0$ such that the solutions of the system $\dot{\xi} = f(\xi(t), u_T(x(kT)), v[k])$ for any $t \in [kT, (k+1)T)$ and $k \in \mathbf{N}_0$ exist and satisfy $|\xi(t)| \le \beta(|\xi(0)|, t) + \gamma(\|v\|_\infty) + d$ for any $t \ge 0$, $T \in (0, T^*)$, $\xi(0) \in \mathbf{R}^n$ with $|\xi(0)| \le D_x$, and $v \in l_\infty$ with $|v| \le D_v$.

III. Circular Path Tracking Control

A. Problem Formulation

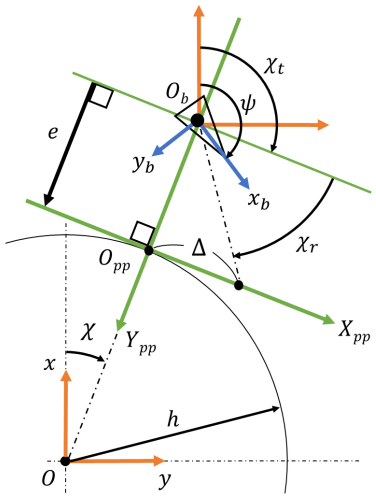

Fig. 1. Circular path and related notation

Consider a four wheeled mobile robot and a designed circular path in Fig. 1 where a robot is represented by a triangular mark and the center and radius of a circular path are the origin of the inertia coordinate systems O-xy and $h > 0$, respectively. The dynamical model of the robot is given by

$$\dot{x} = r\cos\psi, \quad \dot{y} = r\sin\psi, \quad \dot{\psi} = \frac{r}{L}\tan\phi \quad (5)$$

if side slip is not happening ([19], [20]) where $[\,x(t) \quad y(t)\,]^T$ and $\psi(t)$ are the position of the center of mass O_b and the attitude (or yaw angle) of the robot in the inertia coordinate systems O-xy, $r(t)$ is the forward velocity in the body-fixed coordinate systems O_b-x_by_b, $\phi(t)$ is the steering angle, and $L > 0$ is the distance between front and rear wheel axles. A new coordinate systems O_{pp}-$X_{pp}Y_{pp}$ is chosen as in Fig. 1. Let

$$e = h - \sqrt{x^2 + y^2} \quad (6)$$

be a cross-track error that is the minimum distance between the position of the center of mass O_b and the circular path. Let $\chi = \tan^{-1}(y/x)$ and

$$\chi_t = \chi + \pi/2, \quad (\chi_t = \chi - \pi/2) \quad (7)$$

for a clockwise (counter-clockwise) circular motion of the robot. We also choose a look-ahead distance $\Delta > 0$, which is taken as in Fig. 1 and define a LOS angle as follows

$$\chi_r = \tan^{-1}(-e/\Delta), \ \left(\chi_r = \tan^{-1}(e/\Delta)\right) \quad (8)$$

for a clockwise (counter-clockwise) circular motion ([6], [7]). In the remaining of the paper, we discuss a clockwise circular motion, only.

Let r_d be a desired forward velocity and $r(t) = r_d$ for any $t \geq 0$. Then we consider the steering angle $\phi(t)$ as the control input. Let $\chi_t + \chi_r$ be a desired attitude of the robot and $\tilde{\psi} = \psi - (\chi_t + \chi_r)$ a tracking error of the attitude. Then we consider design of steering angle controllers that achieve $\lim_{t\to\infty}(e(t), \tilde{\psi}(t)) = (0, 0)$. For this problem, we assume
B1: There exists $b \in (0, h)$ such that $x^2(t) + y^2(t) \geq b^2$ for any $t \geq 0$,
B2: There exists $a \in (0, \pi/2)$ such that $|\phi(t)| \leq a$ for any $t \geq 0$.
Note that **B1** is needed to guarantee boundedness of $\dot{\tilde{\psi}}$ and **B2** implies steering angle saturation and a restriction of the control input given by the controller. For given $a \in (0, \pi/2)$, let $\sigma_a(x) = a$ for $x > a$, x for $|x| \leq a$, and $-a$ for $x < -a$.

B. Design of Controllers

By (5)-(8), we have

$$\dot{e} = r_d \sin(\tilde{\psi} + \chi_r)(t), \tag{9}$$

$$\dot{\tilde{\psi}} = (r_d/L)[\tan\phi - (l_1 + l_2)](t) \tag{10}$$

where $l_1 = L(x^2 + y^2)^{-1/2}\sin(\psi - \chi)$ and $l_2 = \Delta L(\Delta^2 + e^2)^{-1}\cos(\psi - \chi)$. Since

$$\sin(\tilde{\psi} + \chi_r) = \sin\chi_r + [\cos\chi_r \frac{\sin\tilde{\psi}}{\tilde{\psi}} + \sin\chi_r \frac{\cos\tilde{\psi} - 1}{\tilde{\psi}}]\tilde{\psi},$$

$\sin\chi_r = -e(\Delta^2 + e^2)^{-1/2}$, and $\cos\chi_r = \Delta(\Delta^2 + e^2)^{-1/2}$, we have

$$\dot{e} = -r_d \frac{e}{\sqrt{\Delta^2 + e^2}} + \Pi(e, \tilde{\psi})\tilde{\psi} \tag{11}$$

where

$$\Pi(e, \tilde{\psi}) = r_d[\frac{\Delta}{\sqrt{\Delta^2 + e^2}} \frac{\sin\tilde{\psi}}{\tilde{\psi}} - \frac{e}{\sqrt{\Delta^2 + e^2}} \frac{\cos\tilde{\psi} - 1}{\tilde{\psi}}].$$

Let $T > 0$ be an input sampling period and the steering angle control realized through a zero-order hold, i.e.,

$$\phi(t) = \phi(kT) =: \phi[k]$$

for any $t \in [kT, (k + 1)T)$. Then the Euler model corresponding to the tracking error dynamics (10) and (11) is given by

$$\rho e = (1 - T\frac{r_d}{\sqrt{\Delta^2 + e^2}})e + T\Pi(e, \tilde{\psi})\tilde{\psi}, \tag{12}$$

$$\rho\tilde{\psi} = \tilde{\psi} + T(r_d/L)[\tan\phi - (l_1 + l_2)] \tag{13}$$

where $(e, \tilde{\psi}) = (e, \tilde{\psi})[k]$ and $(\rho e, \rho\tilde{\psi}) = (e, \tilde{\psi})[k + 1]$ for simplicity of notation.

From the Euler model (12) and (13), we set

$$\phi[k] = \sigma_a(\phi_{sf}[k]) \tag{14}$$

where $a > 0$ is the maximal steering angle of a front wheel and

$$\phi_{sf}[k] = \tan^{-1}\left(-c'\tilde{\psi} + l_1 + l_2\right)[k] \tag{15}$$

with arbitrary $c' > 0$. Then the closed-loop Euler model is given by (12) and

$$\rho\tilde{\psi} = (1 - Tc)\tilde{\psi} + Tv \tag{16}$$

where $c = (r_d/L)c' > 0$ and

$$v[k] = (r_d/L)[\tan\sigma_a(\phi_{sf}) - \tan\phi_{sf}][k]. \tag{17}$$

Remark 3.1: The closed-loop Euler model (12) and (16) is equivalent to (12) and

$$\rho\tilde{\psi} = \tilde{\psi} + T[(r_d/L)u + v] \tag{18}$$

with $u[k] = -c'\tilde{\psi}[k]$. Since $v = (r_d/L)[\tan\sigma_a(\phi_{sf}) + c'\tilde{\psi} - l_1 - l_2]$, $|l_1| \leq L/b$, and $|l_2| \leq L/\Delta$, we have $|v[k]| < \infty$ for any $k \in \mathbf{N}_0$ and hence $v \in l_\infty$. It is obvious that $\phi[k] = \sigma_a(\phi_{sf}[k])$ is locally uniformly bounded.

Lemma 3.1: Assume **B1** and **B2**. Then the closed-loop Euler model (12) and (16) is Lyapnnov-SP-ISS.

Proof. Let (D_1, D_2, d) be arbitrary positive real numbers and $(e_{max}, \tilde{\psi}_{max})$ arbitrary positive real numbers satisfying $e_{max}^2 + \tilde{\psi}_{max}^2 \leq D_1^2$. Let $T^* > 0$ be such that

$$T^* = \min\{\Delta/r_d,\ 1/c\} \tag{19}$$

and $T \in (0, T^*)$ arbitrary. Then we have $1 - Tr_d(\Delta^2 + e^2)^{-1/2}$, $1 - Tc \in (0, 1)$.

Let $(e, \tilde{\psi}, v)$ be such that $|e| \leq e_{max}$, $|\tilde{\psi}| \leq \tilde{\psi}_{max}$, $\|v\|_\infty \leq D_2$, and let $V(e) = |e|$, $W(\tilde{\psi}) = \kappa|\tilde{\psi}|$ for the closed-loop Euler model (12) and (16) where κ is a positive real number which is assigned later. Then we have $W(\rho\tilde{\psi}) - W(\tilde{\psi}) \leq -T\kappa c|\tilde{\psi}| + T\kappa|v|$ and

$$\begin{aligned} V(\rho e) - V(e) &\leq -T\frac{r_d}{\sqrt{\Delta^2 + e^2}}|e| + T\left|\Pi(e, \tilde{\psi})\right||\tilde{\psi}| \\ &\leq -T\frac{r_d}{\sqrt{\Delta^2 + e_{max}^2}}|e| + T\left|\Pi(e, \tilde{\psi})\right||\tilde{\psi}|. \end{aligned}$$

Since $\left|\Pi(e, \tilde{\psi})\right| \leq 2r_d$, we obtain

$$V(\rho e) - V(e) \leq -T\frac{r_d}{\sqrt{\Delta^2 + e_{max}^2}}|e| + 2Tr_d|\tilde{\psi}|.$$

Let $\xi = [\,e \quad \tilde{\psi}\,]^T$, $\xi_i = [\,e_i \quad \tilde{\psi}_i\,]^T$, $i = 1, 2$, and $U(\xi) = V(e) + W(\tilde{\psi})$. Then we have $\min\{1, \kappa\}|\xi| \leq U(\xi) \leq \max\{1, \kappa\}|\xi|$, $|U(\xi_1) - U(\xi_2)| \leq \max\{1, \kappa\}[|e_1 - e_2| + \left|\tilde{\psi}_1 - \tilde{\psi}_2\right|] = \max\{1, \kappa\}|\xi_1 - \xi_2|$, and

$$\begin{aligned} U(\rho\xi) - U(\xi) \leq\ & -T\left\{\frac{r_d}{\sqrt{\Delta^2 + e_{max}^2}}|e| + |\tilde{\psi}|\right\} \\ & -T(\kappa c - 1 - 2r_d)|\tilde{\psi}| + T\kappa|v|. \end{aligned}$$

By choosing $\kappa > (2r_d + 1)/c$, we obtain

$$\frac{U(\rho\xi) - U(\xi)}{T} \leq -\min\{\frac{r_d}{\sqrt{\Delta^2 + e_{max}^2}}, 1\}|\xi| + \kappa|v|.$$

Hence by Definition 2.2, the closed-loop Euler model (12) and (16) is Lyapunov-SP-ISS.

Remark 3.2: Note that $T^* > 0$ given by (19) depends on the choice of $V(e) = |e|$ and $W(\tilde{\psi}) = |\tilde{\psi}|$, in the proof of

Lemma 3.1. If we set $V(e) = e^2$ and $W(\tilde{\psi}) = \tilde{\psi}^2$, then we can find another $T^* > 0$, that is larger than (19).

Remark 3.3: The tracking error dynamics corresponding to the Euler model (12) and (16) (or (18)) is given by (11) and $\dot{\tilde{\psi}} = (r_d/L)u(t) + v(t)$ with $u = -c'\tilde{\psi}$. Let $f(\xi, u, v) = [\, -r_d e(\Delta^2 + e^2)^{-1/2} + \Pi(e, \tilde{\psi})\tilde{\psi} \quad (r_d/L)u + v \,]^T$. Then we have $|f(\xi, u, v)| \le r_d \max\{1/\Delta, 2\}|\xi| + (r_d/L)|u| + |v|$ and hence the assumption **A1** is satisfied.

Finally, for the sampled-data robot and its exact model, let

$$\phi(t) = \sigma_a(\phi_{sf}(kT)) \tag{20}$$

for any $t \in [kT,\ (k+1)T)$ be the steering angle control input where $\phi_{sf}(kT)$ is given by (15) with $[k]$ replaced by (kT). Then by Theorem 2.1, Remarks 3.1, 3.3, and Lemma 3.1, we have the following result.

Theorem 3.1: Consider the tracking error dynamics (9) and (10), and assume **B1** and **B2**. Then the closed-loop exact model of (9) and (10) with (14) is SP-ISS. Moreover, the closed-loop sampled-data system (9) and (10) with (20) is SP-ISS.

Now we assume that only the sampled observation

$$y(j) = \xi(jT_m) = [\, e \quad \tilde{\psi} \,]^T\,(jT_m) \tag{21}$$

is available for control where $T_m > 0$ is a fixed measurement sampling period and satisfies $T_m = qT$ for some integer $q \ge 1$. Note that (21) with $T_m = qT$ and $q \ge 1$ reflects the fact that position measurement given by GPS, motion capture systems, and cameras needs more time than generation and transmission of control inputs. In this case, we must estimate the states at input sampling times $t = kT$ to apply the designed controller (14). Then by [21] and [22], we estimate the states by

$$\xi_c[k+1] = \begin{cases} \xi[k+1], & k+1 = jq, \\ F_T^E(\xi_c, \sigma_a(\phi_{sf}(\xi_c)))[k] & \\ \text{with the initialization} & \\ \xi_c[jq] = \xi[jq], & otherwise \end{cases} \tag{22}$$

and construct the control input

$$u[k] = \sigma_a(\phi_{sf}(\xi_c[k])) \tag{23}$$

where $\phi_{sf}(\xi_c[k])$ and $F_T^E(\xi_c, \sigma_a(\phi_{sf}(\xi_c)))[k]$ are given by (14) and (12), (13) with $\xi = [\, e \quad \tilde{\psi} \,]^T$ replaced by ξ_c, respectively. Then by [21] with Lemma 3.1 and Remarks 3.1 and 3.3, we have the following result.

Theorem 3.2: Consider the tracking error dynamics (9) and (10), and assume **B1** and **B2**. Then the closed-loop exact model of (9) and (10) with (21)-(23) is SP-ISS. Moreover, the closed-loop sampled-data system (9) and (10) with (21)-(23) is SP-ISS.

Remark 3.4: 1) In [9], design of circular path following controllers has been discussed for continuous-time two wheeled mobile robots without input saturation by the LOS guidance algorithm. Then uniformly globally asymptotic stability and locally exponential stability of the closed-loop system has been shown by applying the stability theory of cascade systems [23]. Similar to [9], we can design a continuous-time controller

$$\phi(t) = \sigma_a(\phi_{sf}(t)) \tag{24}$$

where $\phi_{sf}(t)$ is given by (15) with $[k]$ replaced by (t). Then the closed-loop system (11) and (10) with (24) is given by

$$\dot{e} = -r_d e(\Delta^2 + e^2)^{-\frac{1}{2}} + \Pi(e, \tilde{\psi})\tilde{\psi}, \quad \dot{\tilde{\psi}} = -c\tilde{\psi} + v \tag{25}$$

where $v(t)$ is given by (17) with $[k]$ replace by (t). By introducing $V(e) = \ln\sqrt{1 + (e^2/\Delta^2)}$ and $W(\tilde{\psi}) = |\tilde{\psi}|$ as Lyapunov candidates, we can show that a cascade system (25) is integral input-to-state stable (iISS) that is slightly weaker stability than ISS ([24], [25]). Although the designed controller (20) coincides with emulation of (24), the proposed controller (20) can guarantee SP-ISS of the sampled-data closed-loop system (9), (10) and (20) by applying the nonlinear sampled-data control theory based on the Euler model.

2) In [13], both single-rate and multi-rate digital controllers for car-like mobile robots without input saturation are designed by extending TFL to sampled-data systems. Since TFL must satisfy some relative degree condition, T-dependent dummy output and dynamic extension are needed for design of single-rate controllers. For multi-rate controllers, we also have a restriction between T and T_m. Compare to [13] our design of controllers based on the LOS guidance algorithm and the Euler model is simple and intuitive.

3) Note that four wheeled mobile robots with steering angle saturation are more general than wheeled mobile robots in [9] and [13].

4) Since we must consider inter-sample behavior of nonlinear sampled-data systems, it is very hard (or sometimes impossible) to guarantee global control performance under mild conditions. But in some practical control systems, behavior of sampled-data control systems is restricted in some region. Hence we propose the semi-global results from a practical point of view. For details, see [11].

IV. Simulation and Experimental Results

We apply the designed single-rate controllers (20) and the multi-rate controllers (21)-(23) to the four wheeled mobile robot "LIMO" developed by Agilex Robotics Co Ltd. Its detailed physical image and English manual are given in [26]. For this robot, $L = 0.2$ [m] and the steering angle is saturated by $|\phi| \le 28$ [deg], ($|\phi| \le 0.49$ [rad]). Its position and attitude of the robot are measured by a ceiling camera and an inertial measurement unit (IMU) equipped in the robot, respectively. Let $h = 1$ [m], $\Delta = 0.25$ [m], and $r_d = 0.2$ $[m/s]$. By simulation and experimental results, we show control performance of the designed controllers and its dependence on a length of input and measurement sampling periods.

First we consider the single-rate controllers (20) with $T = T_m = 0.1$ and 0.5 [sec]. Let $c' = 1.0$ and $(x(0), y(0), \psi(0)) = (1, 2, \pi)$ the initial position and attitude of the robot. Then Figs. 2 and 3 are the experimental results

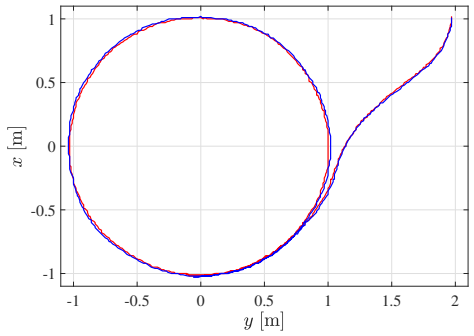

Fig. 2. Trajectories of the robot given by the single-rate controller (20) with $c' = 1$ for $T = 0.1$ (red line) and $T = 0.5$ (blue line)

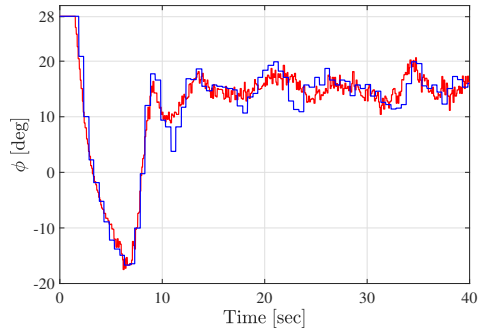

Fig. 3. Time responses of $\phi(t)$ given by the single-rate controller (20) with $c' = 1$ for $T = 0.1$ (red line) and $T = 0.5$ (blue line)

of the trajectories $(x(t), y(t))$ of the robot and the time response of the steering angle control input $\phi(t)$ where red and blue lines correspond to input sampling periods $T = 0.1$ and 0.5 [sec], respectively. Fig. 3 shows no steering saturation except for $t \in (0, 2]$ and hence Figs. 2 and 3 show that the designed controller achieves sampled-data circular path following for both $T = 0.1$ and 0.5 [sec] in the SPAS sense.

Let $c' = 10$ under the same initial position and attitude of the robot. Then the experimental results of $(x(t), y(t))$ and the time responses of $\phi(t)$ are given in Figs. 4 and 5, respectively. Fig. 5 shows the steering angle saturation that is happening continuously and repeatably for both $T = 0.1$ and 0.5 [sec]. In this case the designed single-rate controller (20) with $c' = 10$ achieves sampled-data circular path following in the SP-ISS sense, only. Moreover, we see that offset, which corresponds to error between the robot and the desired circular path, becomes bigger when a length of sampling period becomes longer.

As mentioned in Remark 3.2, although $T^* > 0$ given by (19) in the proof of Lemma 3.1 depends on a choice of Lyapunov functions, we expect that T^* becomes smaller for larger $c' > 0$ by (19) and control performance of the designed single-rate controllers, which is given by Figs. 2-5, is valid.

We also give a comparison of simulation and experimental results of the trajectories for $c' = 10$ and $T = 0.5$ (Fig. 6), where the red solid line and the triangular marks are the

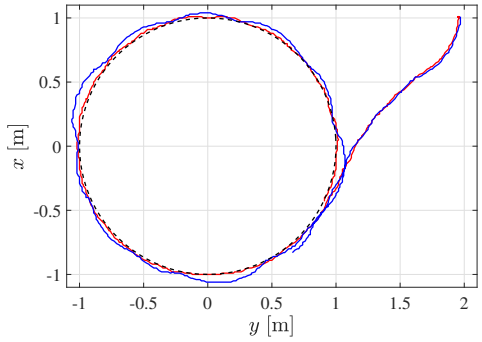

Fig. 4. Trajectories of the robot given by the single-rate controller (20) with $c' = 10$ for $T = 0.1$ (red solid line) and $T = 0.5$ (blue solid line) and the desired circular path (black broken line)

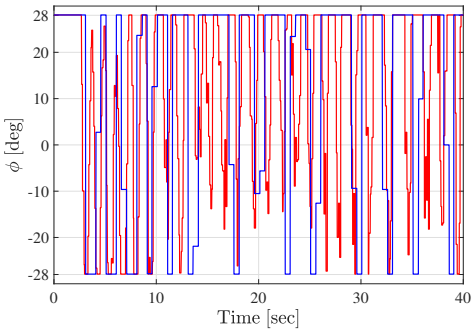

Fig. 5. Trajectories of LIMO given by the single-rate controller (20) with $c' = 10$ for $T = 0.1$ (red line) and $T = 0.5$ (blue line)

experimental result of the trajectory and attitude of the robot at every 6 [sec], the blue solid line is the simulation result of the trajectory, and the black broken line is the desired circular path. Fig. 6 shows that the experimental result is close to the simulation one, although offset of the experimental result is slightly larger than that of the simulation one.

Finally we consider the multi-rate controllers (21)-(23) with $(T, T_m) = (0.1, 1)$. Let $c' = 10$ under the same initial position and attitude of the robot. Then Figs. 7 and 8 show the experimental results of $(x(t), y(t))$ and the time response of $\phi(t)$ given by the multi-rate controller (21)-(23) with $(T, T_m) = (0.1, 1)$ and the single-rate controller (20) with $T = T_m = 1$ where the red and blue lines correspond to the multi-rate and single-rate controllers, respectively and the black broken line is the desired circular path. By Fig. 7 and 8, we can see that the multi-rate controller (21)-(23) with $(T, T_m) = (0.1, 1)$ achieves much better control performance than the single-rate controller (20) with $T = T_m = 1$. Furthermore, Figs. 4 and 7 show that the multi-rate controller (21)-(23) with $(T, T_m) = (0.1, 1)$ attains the control performance recovery of the single-rate controller (20) with $T = T_m = 0.1$.

Videos of the experimental results are also uploaded in `https://www.youtube.com/channel/UCkaqL9f5osPsci8SP9zN7OQ`.

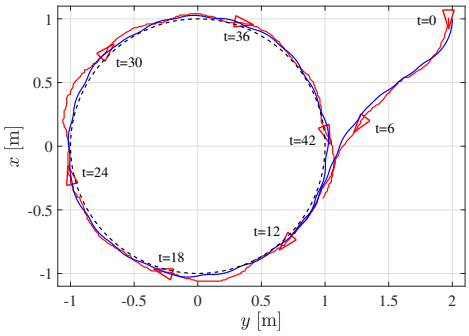

Fig. 6. Trajectories and the attitudes at every 6 [sec] of the robot: Simulation (blue solid line) and experimental (red solid line and triangular marks) results

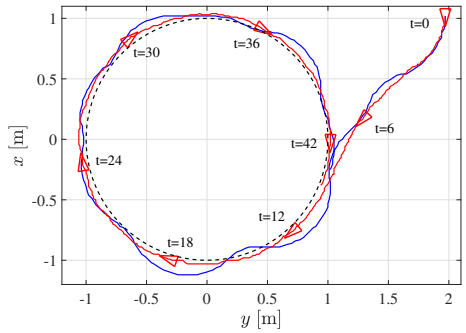

Fig. 7. Trajectories of the robot given by the multi-rate controller (21)-(23) with $c' = 10$, $(T, T_m) = (0.1, 1)$ (red line) and the single-rate controller (20) with $T = 1$ (blue line)

V. Conclusion

In this paper, we have considered the sampled-data circular path following control of four wheeled mobile robots with steering angle saturation. We have designed both single-rate and multi-rate circular path following controllers based on the Euler model of the tracking error dynamics and shown that the closed-loop sampled-data tracking error dynamics is SP-ISS. Moreover, we have illustrated the effectiveness of the designed controllers by simulation and experimental results.

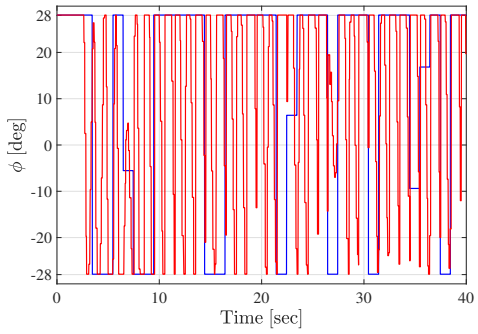

Fig. 8. Time responses of $\phi(t)$ given by the multi-rate controller (21)-(23) with $c' = 10$, $(T, T_m) = (0.1, 1)$ (red line) and the single-rate controller (20) with $T = 1$ (blue line)

References

[1] B. Lantos and L. Márton, *Nonlinear control of vehicles and robots*, ser. Advances in industrial control. Springer, 2011.

[2] Q. Zhihua, *Cooperative control of dynamical systems : applications to autonomous vehicles*. Springer, 2010.

[3] B. Yi, R. Ortega, I. R. Manchester, and H. Siguerdidjane, "Path following of a class of underactuated mechanical systems via immersion and invariance-based orbital stabilization," *International Journal of Robust and Nonlinear Control*, vol. 30, no. 18, pp. 8521–8544, 2020.

[4] O. H. Dagci, U. Y. Ogras, and U. Ozguner, "Path following controller design using sliding mode control theory," *Proceedings of American Control Conference*, pp. 903–908, 2003.

[5] A. Akhtar, C. Nielsen, and S. L. Waslander, "Path following using dynamic transverse feedback linearization for car-like robots," *IEEE Transactions on Robotics*, vol. 31, no. 2, pp. 269–279, 2015.

[6] T. Fossen, M. Breivik, and R. Skjetne, "Line-of-sight path following of underactuated marine craft," *IFAC Proceedings Volumes*, vol. 36, pp. 211–216, 2003.

[7] M. Breivik and T. Fossen, "Path following of straight lines and circles for marine surface vessels," *IFAC Proceedings Volumes*, vol. 37, no. 10, pp. 65–70, 2004.

[8] E. Børhaug, A. Pavlov, E. Panteley, and K. Y. Pettersen, "Straight line path following for formations of underactuated marine surface vessels," *IEEE Transactions on Control Systems Technology*, vol. 19, pp. 493–506, 2011.

[9] M. Breivik and T. Fossen, "Guidance-based path following for wheeled mobile robots," *IFAC Proceedings Volumes*, vol. 38, no. 1, pp. 13–18, 2005.

[10] T. Chen and B. A. Francis, *Optimal sampled-data control systems*, ser. Communications and control engineering. Springer, 1995.

[11] D. S. Laila, D. Nešić, and A. Astolfi, "Sampled-data control of nonlinear systems," *Advanced Topics in Control Systems Theory*, vol. 328, pp. 91–137, 2005.

[12] S. Monaco and D. Normand-Cyrot, "An introduction to motion planning under multirate digital control," *Proceeding of the 1992 IEEE Conference on Decision and Control*, pp. 1780–1785, 1992.

[13] M. Elobaid, M. Mattioni, S. Monaco, and D. Normand-Cyrot, "Digital path following for a car-like robot," *IFAC PapaersOnLine*, vol. 54, no. 21, pp. 174–179, 2021.

[14] H. Katayama and H. Aoki, "Straight-line trajectory tracking control for sampled-data underactuated ships," *IEEE Transactions on Control Systems Technology*, vol. 22, pp. 1638–1645, 2014.

[15] T. I. Fossen, *Marine control systems : guidance, navigation and control of ships, rigs and underwater vehicles*. Marine cybernetics, 2002.

[16] H. K. Khalil, *Nonlinear Systems*, 3rd ed. Prentice Hall, 2002.

[17] D. Nesic and D. Laila, "A note on input-to-state stabilization for nonlinear sampled-data systems," *IEEE Transactions on Automatic Control*, vol. 47, no. 7, pp. 1153–1158, 2002.

[18] D. Nesic, A. R. Teel, and E. D. Sontag, "Formulas relating kl stability estimates of discrete-time and sampled-data nonlinear systems," *Systems and Control Letters*, vol. 38, pp. 49–60, 1999.

[19] P. Mellodge and P. Kachroo, *Model abstraction in dynamical systems : application to mobile robot control*, ser. Lecture notes in control and information sciences. Springer, 2008.

[20] R. M. Murray, Z. Li, and S. S. Sastry, *A Mathematical Introduction to Robotic Manipulation*. CRC Press, 12 2017.

[21] X. Liu, H. J. Marquez, and Y. Lin, "Input-to-state stabilization for nonlinear dual-rate sampled-data systems via approximate discrete-time model," *Automatica*, vol. 44, no. 12, pp. 3157–3161, 2008.

[22] I. G. Polushin and H. J. Marquez, "Multirate versions of sampled-data stabilization of nonlinear systems," *Automatica*, vol. 40, no. 6, pp. 1035–1041, 2004.

[23] A. Loría and E. Panteley, "Cascaded nonlinear time-varying systems: Analysis and design," *Advanced topics in control systems theory*, vol. 311, pp. 23–64, 2005.

[24] A. Chaillet and D. Angeli, "Integral input to state stable systems in cascade," *Systems and Control Letters*, vol. 57, pp. 519–527, 2008.

[25] D. Angeli, E. Sontag, and Y. Wang, "A characterization of integral input-to-state stability," *IEEE Transactions on Automatic Control*, vol. 45, pp. 1082–1097, 2000.

[26] "Limo usage and development manual." [Online]. Available: https://cir.nii.ac.jp/crid/1361137043769898240